Global convergence of quorum-sensing networks

Giovanni Russo[1,*] and Jean Jacques Slotine[2,†]

[1] *Department of Systems and Computer Engineering, University of Naples Federico II, Italy. Work done while visiting the Nonlinear Systems Laboratory, Massachusetts Institute of Technology*
[2] *Nonlinear Systems Laboratory, Massachusetts Institute of Technology, United States*

In many natural synchronization phenomena, communication between individual elements occurs not directly, but rather through the environment. One of these instances is bacterial quorum sensing, where bacteria release signaling molecules in the environment which in turn are sensed and used for population coordination. Extending this motivation to a general nonlinear dynamical system context, this paper analyzes synchronization phenomena in networks where communication and coupling between nodes are mediated by shared dynamical quantities, typically provided by the nodes' environment. Our model includes the case when the dynamics of the shared variables themselves cannot be neglected or indeed play a central part. Applications to examples from systems biology illustrate the approach.

To be published in Physical Review E 82, 2010 (with corrections)

* giovanni.russo2@unina.it
† jjs@mit.edu

I. INTRODUCTION

Many dynamical phenomena in biology involve some form of *synchronization*. Synchronization has attracted much research both from the theoretical, see e.g. [1],[2], [3] to cite just a few, and experimental [4], [5] viewpoints. The particular case of synchronized *time-periodic* processes, where time-scales can range from a few milliseconds to several years [6], [7], includes e.g. circadian rhythms in mammals [8], the cell cycle [9], spiking neurons [10] and respiratory oscillations [11].

When modelling such networks, it is often assumed that each node communicates directly with other nodes in the network, see e.g. [12] [13] and references therein. In many natural instances, however, network nodes do not communicate directly, but rather by means of noisy and continuously changing environments. Bacteria, for instance, produce, release and sense signaling molecules (so-called autoinducers) which can diffuse in the environment and are used for population coordination. This mechanism, known as *quorum sensing* [14], [15], [16] is believed to play a key role in bacterial infection, as well as e.g. in bioluminescence and biofilm formation [17], [18]. In a neuronal context, a mechanism similar to that of quorum sensing may involve *local field potentials*, which may play an important role in the synchronization of groups of neurons [19], [20], [21], [22], [23], [24], [25], [26], or it may occur through a different level in a cortical hierarchy [27], [28], [29], [30], [31]. Other examples of such a mechanism are the synchronization of chemical oscillations of catalyst-loaded reactants in a medium of catalyst-free solution [32], cold atoms interacting with a coherent electromagnetic field [33] and the onset of coordinated activity in a population of micro-organisms living in a shared environment [34], [35].

From a network dynamics viewpoint, the key characteristic of quorum sensing-like mechanisms lies in the fact that communication between nodes (e.g. bacteria) occurs by means of a shared quantity (e.g. the autoinducer concentration), typically in the environment. Furthermore, the production and degradation rates of such a quantity are affected by all the nodes of the network. Therefore, a detailed model of such a mechanism needs to keep track of the temporal evolution of the shared quantity, resulting in an additional set of ordinary differential equations. Such an indirect coupling model has been recently reported in e.g. [36], [37] in the context of periodic oscillations, while in [38] synchronization of two chaotic systems coupled through the environment is investigated. In these papers it is shown that under suitable conditions oscillators can synchronize and that this kind of coupling can lead to a rich variety of synchronous behaviors. In this paper, we will use the generic term "quorum sensing" to describe all such interactions through a shared environmental variable, regardless of the dependence of this variable on the number of network nodes.

Mathematical work on such quorum sensing topologies is relatively sparse (e.g., [39], [21], [40], [36], [37], [38]) compared to that on diffusive topologies, and it often neglects the dynamics of the quorum variables or the environment, as well as the global effects of nonlinearities. This sparsity of results is somewhat surprising given that, besides its biological pervasiveness, quorum sensing may also be viewed as an astute "computational" tool. Specifically, the use of a shared variable in effect significantly reduces the number of links required to achieve a given connectivity [21].

This paper derives novel sufficient conditions for the coordination of nodes communicating through dynamical quorum sensing mechanisms, based on a full nonlinear dynamic analysis. These results can be used both to study natural networks and to guide design of communication mechanisms in synthetic or partially synthetic networks.

After introducing in Section II the basic mathematical tool used in the paper, we start with considering, in Section III A, the case where the network nodes (e.g., the biological entities populating the environment) are all identical or nearly identical. We then focus, in Section III B, on networks composed of heterogeneous nodes, i.e., nodes of possibly diverse dynamics. In this case we provide sufficient conditions ensuring that all the network nodes sharing the same dynamics converge to a common behavior, a particular instance of so-called concurrent synchronization [41], [42]. In Section III C, the results are further extended to a distributed version of quorum sensing, where multiple groups of possibly heterogeneous nodes communicate by means of multiple media. In Section IV, we show that driving the shared environmental variable with an exogenous signal of a given period provides a mechanism for making the network nodes oscillate at the same period. Finally, Section V studies the dependence of synchronization properties on the number of nodes, a question of interest e.g. in the context of cell proliferation. Section VI illustrates the general approach with a set of examples.

Our proofs are based on nonlinear contraction theory ([43]), a viewpoint on incremental stability which we briefly review in Section II, and which has emerged as a powerful tool in applications ranging from Lagrangian mechanics to network control. Historically, ideas closely related to contraction can be traced back to [44] and even to [45] (see also [46], [47], and e.g. [48] for a more exhaustive list of related references). As pointed out in [43], contraction is preserved through a large variety of systems combinations, and in particular it represents a natural tool for the study and design of nonlinear state observers, and by extension, of synchronization mechanisms [49].

II. CONTRACTION THEORY TOOLS

A. Basic results

Recall that, given a norm $|\cdot|$ on the state space, and its induced matrix norm $\|A\|$, for an arbitrary square matrix A, the associated *matrix measure* μ is defined as (see [50], [51])

$$\mu(A) := \lim_{h \to 0^+} \frac{1}{h} \left(\|I + hA\| - 1 \right).$$

The basic result of nonlinear contraction analysis [43] which we shall use in this paper can be stated as follows.

Theorem 1 (Contraction)**.** *Consider the m-dimensional deterministic system*

$$\dot{x} = f(x,t) \tag{1}$$

where f is a smooth nonlinear function. The system is said to be contracting if any two trajectories, starting from different initial conditions, converge exponentially to each other. A sufficient condition for a system to be contracting is the existence of some matrix measure, μ, such that

$$\exists \lambda > 0, \ \forall x, \ \forall t \geq 0, \quad \mu \left(\frac{\partial f(x,t)}{\partial x} \right) \ \leq \ -\lambda \tag{2}$$

The scalar λ defines the contraction rate of the system.

The standard matrix measures used in this paper are listed in Table I. More generally, contraction may be shown by using matrix measures induced by the weighted vector norm $|x|_{\Theta,i} = |\Theta x|_i$, with Θ a constant invertible matrix and $i = 1, 2, \infty$. Such measures, denoted with $\mu_{\Theta,i}$, are linked to the standard measures by:

$$\mu_{\Theta,i}(A) = \mu_i \left(\Theta A \Theta^{-1} \right), \quad \forall i = 1, 2, \infty$$

In this paper, Θ will be either the identity or a diagonal matrix. Note that for linear time-invariant systems, contraction is equivalent to strict stability, and, using the Euclidean vector norm, Θ can be chosen as the transformation matrix which diagonalizes the system or puts it in Jordan form [43].

TABLE I. Standard matrix measures for a real $n \times n$ matrix, $A := [a_{ij}]$. The i-th eigenvalue of A is denoted with $\lambda_i(A)$.

vector norm, $\|\cdot\|$	induced matrix measure, $\mu(A)$
$\|x\|_1 = \sum_{j=1}^n \|x_j\|$	$\mu_1(A) = \max_j \left(a_{jj} + \sum_{i \neq j} \|a_{ij}\| \right)$
$\|x\|_2 = \left(\sum_{j=1}^n \|x_j\|^2 \right)^{\frac{1}{2}}$	$\mu_2(A) = \max_i \left(\lambda_i \left\{ \frac{A + A^*}{2} \right\} \right)$
$\|x\|_\infty = \max_{1 \leq j \leq n} \|x_j\|$	$\mu_\infty(A) = \max_i \left(a_{ii} + \sum_{j \neq i} \| \ a_{ij} \ \| \right)$

For convenience, in this paper we will also say that a *function* $f(x,t)$ is contracting if the system $\dot{x} = f(x,t)$ satisfies the sufficient condition above. Similarly, we will then say that the corresponding Jacobian *matrix* $\frac{\partial f}{\partial x}(x,t)$ is contracting.

We shall also use the following two properties of contracting systems, whose proofs can be found in [43], [52].

Hierarchies of contracting systems Assume that the Jacobian of (1) is in the form

$$\frac{\partial f}{\partial x}(x,t) \ = \ \begin{bmatrix} J_{11} & J_{12} \\ 0 & J_{22} \end{bmatrix} \tag{3}$$

corresponding to a hierarchical dynamic structure. The J_{ii} may be of different dimensions. Then, a sufficient condition for the system to be contracting is that (i) the Jacobians J_{11}, J_{22} are contracting (possibly with different Θ's and for different matrix measures), and (ii) the matrix J_{12} is bounded.

Periodic inputs Consider the system

$$\dot{x} = f(x, r(t)) \tag{4}$$

where the input vector $r(t)$ is periodic, of period T. Assume that the system is contracting (i.e., that the Jacobian matrix $\frac{\partial f}{\partial x}(x, r(t))$ is contracting for any $r(t)$). Then the system state $x(t)$ tends exponentially towards a periodic state of period T.

B. Partial Contraction

A simple yet powerful extension to nonlinear contraction theory is the concept of *partial* contraction [49].

Theorem 2 (Partial contraction)**.** *Consider a smooth nonlinear m-dimensional system of the form $\dot{x} = f(x, x, t)$ and assume that the so-called virtual system $\dot{y} = f(y, x, t)$ is contracting with respect to y. If a particular solution of the auxiliary y-system verifies a smooth specific property, then all trajectories of the original x-system verify this property exponentially. The original system is said to be* partially contracting.

Indeed, the virtual y-system has two particular solutions, namely $y(t) = x(t)$ for all $t \geq 0$ and the particular solution with the specific property. Since all trajectories of the y-system converge exponentially to a single trajectory, this implies that $x(t)$ verifies the specific property exponentially.

C. Networks of contracting nodes

This section introduces preliminary results on concurrent synchronization of networks, which will be used in the rest of the paper.

We now consider a network where its $N > 1$ nodes may have different dynamics (in the rest of the paper, we will say that nodes are heterogeneous):

$$\dot{x}_i = f_{\gamma(i)}(x_i, t) + \sum_{j \in N_i} \left[h_{\gamma(i)}(x_j) - h_{\gamma(i)}(x_i) \right] \tag{5}$$

where N_i denotes the set of neighbors of node i and γ is a function defined between two set of indices (not necessarily a permutation), i.e.

$$\gamma : \{1, \ldots, N\} \to \{1, \ldots, s\} \quad s \leq N \tag{6}$$

Thus, two nodes of (5), e.g. x_i and x_j, share the same dynamics and belong to the p-th group (denoted with $\mathcal{G}_p$), i.e. $x_i, x_j \in \mathcal{G}_p$, if and only if $\gamma(i) = \gamma(j) = p$. The dimension of the nodes' state variables belonging to group p is $n_{\gamma(i)}$, i.e. $x_i \in \mathbb{R}^{n_{\gamma(i)}}$ for any $x_i \in \mathcal{G}_p$. In what follows we assume that the Jacobian of the coupling functions $h_{\gamma(i)}$ are diagonal matrices with nonnegative diagonal elements. We will derive conditions ensuring *concurrent synchronization* of (5), i.e. all nodes belonging to the same group exhibit the same regime behavior.

In what follows the following standard assumption (see [41] and references therein) is made on the interconnections between the agents belonging to different groups, [53].

Definition 1. *Let i and j be two nodes of a group G_p, receiving their input from elements i', j' respectively, with: (i) i' and j' belonging to the same group $G_{p'}$; (ii) the coupling functions between i-i' and j-j' being the same; (iii) the inputs to i and j coming from different groups are the same. If these assumptions are satisfied, then nodes i and j are said to be* input-equivalent.

Given this definition, we can state the following theorem, which generalizes results in [41] to the case of arbitrary norms. Its proof is provided in the Appendix.

Theorem 3. *Assume that in (5) the nodes belonging to the same group are all input-equivalent and that the nodes dynamics are all contracting. Then, all node trajectories sharing the same dynamics converge towards each other, i.e. for any x_i, $x_j \in \mathcal{G}_p$, $p = 1, \ldots, s$,*

$$|x_j(t) - x_i(t)| \to 0 \quad \text{as} \quad t \to +\infty$$

In the case of networks of identical nodes dynamics, the above result amounts to only requiring contraction for each node.

III. MAIN RESULTS

In this section, we first provide sufficient conditions for the synchronization of a network composed of N nodes communicating over a common medium, itself characterized by some nonlinear dynamics. We then extend the analysis by providing sufficient conditions for the convergence of networks composed of nodes having different dynamics (non-homogeneous nodes), or communicating over multiple (possibly non-homogeneous) media.

A. The basic mathematical model and convergence analysis

In the following, we analyze the convergent behavior of networks of nodes which are globally coupled through a shared quantity (often, the environment) see Figure 1 (left). In such a network, the N nodes are assumed be all identical, i.e. to all share the same smooth dynamics, and to communicate by means of the same common medium, also characterized by some smooth dynamics:

$$\begin{aligned} \dot{x}_i &= f\left(x_i, z, t\right) && i = 1, \ldots, N \\ \dot{z} &= g\left(z, \Psi\left(x_1, \ldots, x_N\right), t\right) \end{aligned} \tag{7}$$

A simplified version of the above model was recently analyzed by means of a graphical algorithm in [54]. In the above equation, the set of state variables of the nodes is x_i, while the set of the state variables of the common medium dynamics is z. Notice that the nodes dynamics and the medium dynamics can be of different dimensions (e.g. $x_i \in \mathbb{R}^n$, $z \in \mathbb{R}^d$). The dynamics of the nodes affect the dynamics of the common medium by means of some (coupling, or input) function, $\Psi : \mathbb{R}^{Nn} \to \mathbb{R}^d$. These functions may depend only on some of the components of the x_i or of z (as the example in Section VI B illustrates).

The following result is a sufficient condition for convergence of all nodes trajectories of (7) towards each other.

Theorem 4. *All nodes trajectories of network (7) globally exponentially converge towards each other if the function $f\left(x, v(t), t\right)$ is contracting for any $v(t) \in \mathbb{R}^d$.*

Proof. The proof is based on partial contraction (Theorem 2). Consider the following *reduced order* virtual system

$$\dot{y} = f\left(y, z, t\right) \tag{8}$$

Notice that now $z(t)$ is an exogenous input to the virtual system. Furthermore, substituting x_i to the virtual state variable y yields the dynamics of the i-th node. That is, x_i, $i = 1, \ldots, N$, are particular solutions of the virtual system. Now, if such a system is contracting, then all of its solutions will converge towards each other. Since the nodes state variables are particular solutions of (8), contraction of the virtual system implies that, for any $i, j = 1, \ldots, N$:

$$|x_i - x_j| \to 0 \text{ as } \ t \to +\infty$$

The Theorem is proved by noting that by hypotheses the function $f(x, v(t), t)$ is contracting for any exogenous input $v(t)$. This in particular implies that $f(y, z, t)$ is contracting, i.e. (8) is contracting. □

Remarks

- In the case of diffusive-like coupling between nodes and the common medium, system (7) reduces to:

$$\begin{aligned} \dot{x}_i &= f\left(x_i, t\right) + k_z\left(z\right) - k_x\left(x_i\right) && i = 1, \ldots, N \\ \dot{z} &= g\left(z, t\right) + \textstyle\sum_{i=1}^{N} \left[u_x\left(x_i\right) - u_z\left(z\right)\right] \end{aligned} \tag{9}$$

  That is, the nodes and the common medium are coupled by means of the smooth functions $k_z : \mathbb{R}^d \to \mathbb{R}^n$, $k_x : \mathbb{R}^n \to \mathbb{R}^n$ and $u_x : \mathbb{R}^n \to \mathbb{R}^d$, $u_z : \mathbb{R}^d \to \mathbb{R}^d$. These functions may depend only on some of the components of the x_i or of z (as we shall illustrate in Section VI B). Theorem 4 implies that synchronization is attained if $f\left(x, t\right) - k_x\left(x\right)$ is contracting. Similar results are easily derived for the generalizations of the above model presented in what follows.

- The result also applies to the case where the quorum signal is based not on the x_i's themselves, but rather on variables deriving from the x_i's through some further nonlinear dynamics. Consider for instance the system

$$\begin{aligned} \dot{x}_i &= f\left(x_i, z, t\right) && i = 1, \ldots, N \\ \dot{r}_i &= h\left(r_i, x_i, z, t\right) && i = 1, \ldots, N \\ \dot{z} &= g\left(z, \Psi\left(r_1, \ldots, r_N\right), t\right) \end{aligned}$$

  Theorem 4 can be applied directly by describing each network node by the augmented state (x_i, r_i), and using property (3) on hierarchical combinations to evaluate the contraction properties of the augmented network dynamics.

- Similarly, each network "node" may actually be composed of several subsystems, with each subsystem synchronizing with its analogs in other nodes.
- As in previous contraction work, the individual node dynamics are quite general, and could describe e.g. neuronal oscillator models as well as bio-chemical reactions. In the case that the individual node dynamics represents a system with multiple equilibria, then synchronization corresponds to a common "vote" for a particular equilibrium.
- A condition for synchronization weaker than Theorem 4 is that the function $f(x,v,t)$ be contracting only for some values of v, i.e. $v \in V \subset \mathbb{R}^d$. In this case, the medium dynamics acts as a switch which activates/deactivates synchronization according to the values of z.

B. Multiple systems communicating over a common medium

We now generalize the mathematical model analyzed in the previous Section, by allowing for $s \leq N$ groups (or clusters) of nodes characterized by different dynamics (with possibly different dimensions) to communicate over the same common medium (see Figure 1, right). We will prove a sufficient condition for the global exponential convergence of all nodes trajectories belonging to the same group towards each other. This regime is called concurrent synchronization [41].

The mathematical model analyzed here is

$$\begin{aligned} \dot{x}_i &= f_{\gamma(i)}\left(x_i, z, t\right) \\ \dot{z} &= g\left(z, \Psi\left(x_1, \ldots, x_N\right), t\right) \end{aligned} \tag{10}$$

where: i) γ is defined as in (6); ii) x_i denotes the state variables of the network nodes (nodes belonging to different groups may have different dimensions, say $n_{\gamma(i)}$) and z denotes the state variables for the common medium ($z \in \mathbb{R}^d$); iii) Ψ, defined analogously to the previous Section, denotes the coupling function of the group $\gamma(i)$ with the common medium dynamics ($\Psi : \mathbb{R}^{n_{\gamma(1)}} \times \ldots \times \mathbb{R}^{n_{\gamma(N)}} \to \mathbb{R}^d$).

Theorem 5. *Concurrent synchronization is achieved in network (10) if the functions $f_{\gamma(i)}\left(x, v(t), t\right)$ are all contracting for any $v(t) \in \mathbb{R}^d$.*

Proof. Recall that (10) is composed by N nodes having dynamics $f_1, \ldots, f_s$. Now, in analogy with the proof of Theorem 4, consider the following virtual system:

$$\begin{aligned} \dot{y}_1 &= f_1\left(y_1, z, t\right) \\ \dot{y}_2 &= f_2\left(y_2, z, t\right) \\ &\vdots \\ \dot{y}_s &= f_s\left(y_s, z, t\right) \end{aligned} \tag{11}$$

where $z(t)$ is seen as an exogenous input to the virtual system. Let $\{X_i\}$ be the set of state variables belonging to the i-th group composing the network, and denote with $X_{i,j}$ any element of $\{X_i\}$. We have that $(X_{1,j}, \ldots, X_{s,j})$ are particular solutions of the virtual system. Now, contraction of the virtual system implies that all of its particular solutions converge towards each other, which in turn implies that all the elements within the same group $\{X_i\}$ converge towards each other. Thus, contraction of the virtual system (11) implies concurrent synchronization of the real system (10).

To prove contraction of (11), compute its Jacobian,

$$J = \begin{bmatrix} \frac{\partial f_1(y_1,z,t)}{\partial y_1} & 0 & 0 & \ldots & 0 \\ 0 & \frac{\partial f_2(y_2,z,t)}{\partial y_2} & 0 & \ldots & 0 \\ \ldots & \ldots & \ldots & \ldots & \ldots \\ 0 & 0 & 0 & 0 & \frac{\partial f_s(y_s,z,t)}{\partial y_s} \end{bmatrix}$$

Now, by hypotheses, we have that all the functions $f_i(x, v(t), t)$ are contracting for any exogenous input. This in turn implies that the virtual system (11) is contracting, since its Jacobian matrix is block diagonal with diagonal blocks being contracting. □

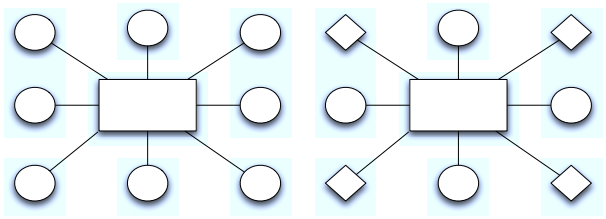

FIG. 1. A schematic representation of networks analyzed in Section III A (left) and Section III B (right). The nodes denoted with circles have a different dynamics from those indicated with squares. The dynamics of the common media is denoted with a rectangle. In our models, the dynamics of the common media is affected by the nodes state variables: this implements a feedback.

C. Systems communicating over different media

In the previous Section, we considered networks where some (possibly heterogeneous) nodes communicate over a common medium. We now consider a *distributed* version of such topology, where each of the $s \leq N$ groups composing the network have a private medium. Communication between the groups is then obtained by coupling only their media (see Figure 2). The objective of this Section, is to provide a sufficient condition ensuring (concurrent) synchronization of such network topology.

Note that the network topology considered here presents a layer structure. In analogy with the terminology used for describing the topology of the Internet and World-Wide-Web (see e.g. [55], [56]), we term as *medium* (or private) level the layer consisting of the nodes of the network and their corresponding (private) media; we then term as *autonomous* level, the layer of the interconnections between the media. That is, the autonomous level is an *abstraction* of the network, having nodes which consist of both the network nodes and their private medium. This in turn implies that in order for two nodes of the autonomous level to be identical they have to share: i) the same dynamics and number of nodes; ii) the same medium dynamics (see Figure 2).

In what follows we will denote with $\mathcal{G}_p$ the set of homogeneous nodes communicating over the medium z_p. We will denote with N_p the set of media which are linked to the medium z_p. Each medium communicates with its neighboring media diffusively. The mathematical model is then:

$$\begin{array}{ll} \dot{x}_i = f_p\left(x_i, z_p, t\right) & x_i \in \mathcal{G}_p \\ \dot{z}_p = g_p\left(z_p, \Psi\left(X_p\right), t\right) + \sum_{j \in N_p}\left[\phi_p\left(z_j\right) - \phi_p\left(z_p\right)\right] & x_i \in \mathcal{G}_p \end{array} \tag{12}$$

where $p = 1, \ldots, s$ and X_p is the stack of all the vectors $x_i \in \mathcal{G}_p$. We assume that the dynamical equations for the media have all the same dimensions (e.g. $z_p \in R^d$), while the nodes belonging to different groups can have different dimensions (e.g. $x_i \in \mathbb{R}^p$, for any $i \in \mathcal{G}_p$). Here, the coupling functions between the media, $\phi_p : \mathbb{R}^d \to \mathbb{R}^d$, are assumed to be continuous and to have a diagonal Jacobian matrix with diagonal elements being nonnegative and bounded. All the matrices $\partial f_p / \partial z$ are assumed to be bounded.

Theorem 6. *Concurrent synchronization is attained in network (12) if: i) the nodes of its* autonomous *level sharing the same dynamics are input-equivalent; ii) $f_p\left(x_i, v(t), t\right)$, $g_p\left(z_p, v(t), t\right)$ are all contracting functions for any $v(t) \in \mathbb{R}^d$; iii) $\frac{\partial f_p}{\partial z_p}$ are all uniformly bounded matrices.*

Proof. Consider the following $2s$-dimensional virtual system, analogous to the one used for proving Theorem 5:

$$\begin{array}{l} \dot{y}_{1,p} = f_p\left(y_{1,p}, y_{2,p}, t\right) \\ \dot{y}_{2,p} = g_p\left(y_{2,p}, v_p(t), t\right) + \sum_{k \in N_p}\left[\phi_p\left(y_{2,k}\right) - \phi_p\left(y_{2,p}\right)\right] \end{array} \tag{13}$$

where $p = 1, \ldots, s$, and $v_p(t) := \Psi\left(X_p\right)$. Notice that the above system is constructed in a similar way as (11). In particular, solutions of (12) are particular solutions of the above virtual system (see the proof of Theorem 5). That is, if concurrent synchronization is attained for (13), then all the nodes sharing the same dynamics will converge towards each other. Now, Theorem 3 implies that concurrent synchronization is attained for system (13) if: i) its nodes are contracting; ii) the coupling functions have a nonnegative bounded diagonal Jacobian; iii) nodes sharing the same dynamics are input equivalent. Since the last two conditions are satisfied by hypotheses, we have only to

prove contraction of the virtual network nodes. Differentiation of nodes dynamics in (13) yields the Jacobian matrix

$$\begin{bmatrix} \frac{\partial f_p(y_{1,p},y_{2,p},t)}{\partial y_{1,p}} & \frac{\partial f_p(y_{1,p},y_{2,p},t)}{\partial y_{2,p}} \\ 0 & \frac{\partial g_p(y_{1,p},v_i(t),t)}{\partial y_{2,p}} \end{bmatrix}$$

The above Jacobian has the structure of a hierarchy. Thus (see Section II) the virtual system is contracting if: (i) $\frac{\partial f_p(y_{1,p},y_{2,p},t)}{\partial y_{1,p}}$ and $\frac{\partial g_p(y_{2,p},v_i(t),t)}{\partial y_{2,p}}$ are both contracting; (ii) $\frac{\partial f_p(y_{1,p},y_{2,p},t)}{\partial y_{2,p}}$ is bounded.

The above two conditions are satisfied by hypotheses. Thus, the virtual network achieves concurrent synchronization (Theorem 3). This proves the Theorem. □

Note that Theorems 4 and 5 do not make any hypotheses on the medium dynamics − synchronization (or concurrent synchronization) can be attained by the network nodes independently of the particular dynamics of the single medium, provided that the function f (or the f_i's) is contracting. By contrast, Theorem 6 shows that the media dynamics becomes a key element for achieving concurrent synchronization in networks where different groups communicate over different media.

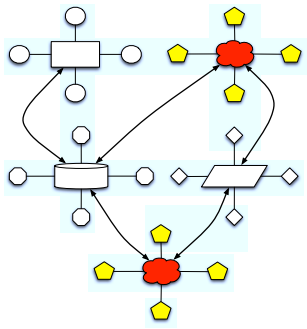

FIG. 2. (Color online) A schematic representation of the network analyzed Section III C. The connections between media (and hence the connections of the autonomous level) are pointed out. Notice that only two nodes of the autonomous level are input equivalent (also pointed out in the Figure) since: i) their media have the same dynamics; ii) both media are shared by the same number of nodes, which have the same dynamics.

Finally, note that all of the above results also allow dimensionality reduction in the analysis of the system's final behavior by treating each group as a single element, similarly to [57], a point we will further illustrate in Section V.

IV. CONTROL OF PERIODICITY

The objective of this section is to provide a sufficient condition to guarantee that the common node behavior, towards which all network nodes globally converge, is oscillatory and exhibits a specified *period*. This is obtained by driving the environmental dynamics with an exogenous signal of the given period. A related problem has been recently addressed in [58], where entrainment of individual contracting biological systems to periodic inputs was analyzed. In our context, the role of the bilateral interaction between nodes and shared environmental variable becomes central.

Our main result, which we shall extend later in the section, is as follows.

Theorem 7. *Consider the following network*

$$\begin{aligned} \dot{x}_i &= f(x_i, z) \qquad\qquad i = 1, \ldots, N \\ \dot{z} &= g(z, \Psi(x_1, \ldots, x_N)) + r(t) \end{aligned} \tag{14}$$

where $r(t)$ is a T-periodic signal. All the nodes of the network synchronize onto a periodic orbit of period T, say $x_T(t)$, if:

- *$f(x_i, v(t))$ is a contracting function;*
- *the reduced order system ($x_c(t) \in \mathbb{R}^n$)*

$$\begin{aligned} \dot{x}_c &= f(x_c, z) \\ \dot{z} &= g(z, \Psi(x_c, \ldots, x_c)) + r(t) \end{aligned}$$

is contracting.

Note that the dynamics f and g include the coupling terms between nodes and environment.

Proof. Consider the virtual system

$$\dot{y}_1 = f(y_1, z) \tag{15}$$

By hypotheses (15) is contracting and hence the nodes state variables will converge towards each other, i.e. $|x_i - x_j| \to 0$ as $t \to +\infty$. That is, all the network trajectories converge towards a unique common solution, say $x_c(t)$. This in turn implies that, after transient, network dynamics are described by the reduced order system

$$\begin{aligned} \dot{x}_c &= f(x_c, z) \\ \dot{z} &= g(z, \Psi(x_c, \ldots, x_c)) + r(t) \end{aligned}$$

Now, the above system is contracting by hypotheses and $r(t)$ is a T periodic signal. In turn, this implies that all of its solutions will converge towards a unique T periodic solution, i.e.

$$|x_c(t) - x_T(t)| \to 0, \qquad t \to +\infty$$

This proves the result. □

System (14) can be thought of as a dynamical system built upon a bidirectional interaction between nodes and medium, and forced by a periodic input. In this view, the conditions of Theorem 7 guarantee global exponential synchronization of the network nodes onto a periodic orbit of the same period as the input, without requiring contraction of either the nodes or the overall dynamics. And indeed, the proof of the Theorem is based on contraction of an appropriately constructed *virtual* system, a much weaker condition. In this sense, our result provides a generalization of the basic result on global entrainment to periodic inputs discussed in Section II A.

Theorem 7 can be extended to the more general case of networks of non-homogeneous nodes communicating over non-homogeneous media.

Theorem 8. *Consider the following network*

$$\begin{array}{ll} \dot{x}_i = f_p(x_i, z_p) & x_i \in \mathcal{G}_p \\ \dot{z}_p = g_p(z_p, \Psi(X_p)) + \sum_{k \in N_p} [\phi(z_k) - \phi(z_p)] + r(t) & x_j \in \mathcal{G}_p \end{array} \tag{16}$$

where X_p is the stack of all the $x_i \in \mathcal{G}_p$ and $r(t)$ is a T-periodic signal. Concurrent synchronization is attained, with a final behavior periodic behavior of period T if:

1. *the nodes of the autonomous level sharing the same dynamics are input equivalent;*

2. *the coupling functions ϕ have bounded diagonal Jacobian with nonnegative diagonal elements;*

3. *$f_p(x_i, v(t))$ are contracting functions for any $v(t) \in \mathbb{R}^d$;*

4. *the reduced order systems ($x_{c,i} \in \mathbb{R}^{n_i}$)*

$$\begin{aligned} \dot{x}_{c,i} &= f_p(x_{c,i}, z_p) \\ \dot{z}_p &= g_p(z_p, \Psi(x_{c,i}, \ldots, x_{c,i})) \end{aligned}$$

are all contracting.

Proof. The proof is formally the same as that of Theorem 6 and Theorem 7, and it is omitted here for the sake of brevity. □

A simple example

Consider a simple biochemical reaction, consisting of a set of $N > 1$ enzymes sharing the same substrate. We denote with $X_1, \dots, X_N$ the concentration of the reaction products. We also assume that the dynamics of S is affected by some T-periodic input, $r(t)$. We assume that the total concentration of X_i, i.e. $X_{i,T}$, is much less than the initial substrate concentration, S_0. In these hypotheses, a suitable mathematical model for the system is given by (see e.g. [59]):

$$\begin{array}{ll} \dot{X}_i = -aX_i + \frac{K_1 S}{K_2+S} & i = 1, \dots, N \\ \dot{S} = -\sum_{i=1}^{N} \frac{K_1 S}{K_2+S} + r(t) & \end{array} \tag{17}$$

with K_1 and K_2 be positive parameters. Thus, a suitable virtual system for the network is

$$\begin{array}{l} \dot{y}_1 = -ay_1 + \frac{K_1 y_2}{K_2+y_2} \\ \dot{y}_2 = -\sum_{i=1}^{N} \frac{K_1 y_2}{K_2+y_2} + r(t) \end{array} \tag{18}$$

Differentiation of the above system yields the Jacobian matrix

$$\begin{bmatrix} -a & \frac{K_2}{(K_2+y_1)^2} \\ 0 & -N\frac{K_2}{(K_2+y_1)^2} \end{bmatrix} \tag{19}$$

It is straightforward to check that the above matrix represents a contracting hierarchy (recall that biochemical parameters are all positive). Thus, all the trajectories of the virtual system globally exponentially converge towards a unique T-periodic solution. This, in turn, implies that X_i, $i = 1, \dots, N$, globally exponentially converge towards each other and towards the same periodic solution.

Figure 3 illustrates the behavior for $N = 3$. Notice that, as expected from the above theoretical analysis, X_1, X_2 and X_3 synchronize onto a periodic orbit of the same period as $r(t)$.

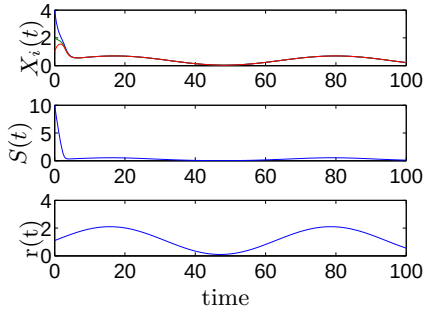

FIG. 3. (Color online) Simulation of (17), with $N = 3$ and $r(t) = 1.1 + \sin(0.1t)$. System parameters are set as follows: $a = 1$, $K_2 = 1$, $K_1 = 2$.

Finally, a simple sufficient condition ensuring contraction of the reduced-order system in Theorem 7 can be obtained when: (i) the intrinsic dynamics of the shared variable is contracting, with contraction rate c_z; (ii) the coupling is diffusive with the Jacobian of the coupling terms being diagonal, i.e. network dynamics is of the same form as (9). Indeed, the Jacobian matrix of the reduced order system is

$$J = \begin{bmatrix} \frac{\partial f}{\partial x_c} - \frac{\partial k}{\partial x_c} & \frac{\partial k}{\partial z} \\ N\frac{\partial u}{\partial x_c} & \frac{\partial g}{\partial x_c} - N\frac{\partial u}{\partial z} \end{bmatrix}$$

Now, the reduced order system is contracting if

$$\begin{array}{l} \mu\left(\frac{\partial f}{\partial x_c} - \frac{\partial k}{\partial x_c}\right) + \frac{\theta_1}{\theta_2}\left\|\frac{\partial k}{\partial z}\right\| \\ \mu\left(\frac{\partial g}{\partial x_c} - N\frac{\partial u}{\partial z}\right) + \frac{\theta_2}{\theta_1}\left\|N\frac{\partial u}{\partial x_c}\right\| \end{array} \tag{20}$$

are both uniformly negative (see Lemma 1). It can be easily shown that this condition is always achieved if the number of nodes is sufficiently large, $N > c_z/\mu\left(\frac{\partial u}{\partial x_c}\right)$.

We also remark here that the reduced order system is contracting if both nodes and medium intrinsic dynamics are contracting (this result is similar to the one obtained in [49] for diffusively coupled networks).

V. EMERGENT PROPERTIES AS N INCREASES

In this Section, we analyze how the convergence properties of a given quorum sensing network vary as the number N of nodes increases. We show that for some typical quorum sensing networks, as N becomes sufficiently large, synchronization always occurs. One particular modeling context where these results have important implications is that of cell proliferation in biological systems.

A. A lower bound on N ensuring synchronization

It is well known [49] that for all-to-all diffusively coupled networks of the form

$$\dot{x}_i = f(x_i, t) + \sum_{i=1}^{N} k(x_j - x_i) \tag{21}$$

the minimum coupling gain k required for synchronization is inversely proportional to the number of nodes composing the network. That is,

$$k_{\min} \propto \frac{1}{N}$$

We now show that a similar bound holds for nodes coupled by means of quorum sensing of the form

$$\begin{aligned} \dot{x}_i &= f\left(x_i, t\right) + kN(z - x_i) \qquad i = 1, \ldots, N \\ \dot{z} &= g\left(z, \Psi(x_1, \ldots, x_N), t\right) \end{aligned} \tag{22}$$

To simplify notations, the above model assumes that z and all x_i have the same dimensions. In addition, the coupling strength increases with the number of nodes N, a frequent property of actual networks based on quorum sensing mechanisms, such as e.g. bacteria proliferation [16] or local field potentials.

Theorem 9. *Assume that the Jacobian* $\left(\frac{\partial f}{\partial x}\right)$ *is upper-bounded by* α *for some matrix measure* μ*, i.e.,*

$$\exists \alpha \in \mathbb{R},\ \forall x,\ \forall t \geq 0, \qquad \mu\left(\frac{\partial f}{\partial x}\right) \leq \alpha$$

Then, network (22) synchronizes if

$$k > \frac{\alpha}{N}$$

That is, $k_{\min} \propto 1/N$.

Proof. Consider the virtual system

$$\dot{y} = f(y, t) + kN(z - y) \tag{23}$$

Synchronization is attained if the virtual system is contracting. Now, computing the matrix measure of the Jacobian of (23) yields for any x and for any $t \geq 0$

$$\mu\left(\frac{\partial f}{\partial y} - kNI\right) \ \leq \ \mu\left(\frac{\partial f}{\partial y}\right) + kN\mu\left(-I\right) \ \leq \ \alpha - kN$$

Thus, the virtual system is contracting if $k > \frac{\alpha}{N}$. □

B. Dependence on initial conditions

We now consider the basic quorum sensing model (7). We derive simple conditions for the final behavior of the network to become independent of initial conditions (in the nodes and the medium) as N becomes large.

Theorem 10. *Assume that for (7) the following conditions hold: (i)* $\mu\left(\frac{\partial f}{\partial x}\right) \to -\infty$ *as* $N \to +\infty$*; (ii)* $g\left(z, v_2(t), t\right)$ *is contracting (for any* $v_2(t)$ *in* $\mathbb{R}^d$*); (iii)* $\left\|\frac{\partial f}{\partial z}\right\|$ *and* $\left\|\frac{\partial g}{\partial v_2}\right\|$ *are bounded for any* x*,* z*,* v_2 *(where* $\|\cdot\|$ *is the operator norm).*

Then, there exists some N^* *such that for any* $N \geq N^*$ *all trajectories of (7) globally exponentially converge towards a unique synchronized solution, independent of initial conditions.*

Proof. We know that contraction of $f\left(x, v_1(t), t\right)$ for any $v_1(t)$ (which the first condition implies for N large enough) ensures network synchronization. That is, there exists a unique trajectory, $x_s(t)$, such that, as $t \to +\infty$,

$$|x_i - x_s| \to 0, \quad \forall i$$

Therefore, the final behavior is described by the following lower-dimensional system:

$$\begin{aligned} \dot{x}_s &= f\left(x_s, z, t\right) \\ \dot{z} &= g\left(z, \Psi\left(x_s\right), t\right) \end{aligned} \tag{24}$$

If in turn this reduced-order system (24) is contracting, then its trajectories globally exponentially converge towards a unique solution, say $x_s^*(t)$, regardless of initial conditions. This will prove the Theorem (similar strategies are extensively discussed in [57]).

To show that (24) is indeed contracting, compute its Jacobian matrix,

$$\begin{bmatrix} \frac{\partial f}{\partial x_s} & \frac{\partial f}{\partial z} \\ \frac{\partial g}{\partial x_s} & \frac{\partial g}{\partial z} \end{bmatrix}$$

Lemma 1 in the Appendix shows that the above matrix is contracting if there exists some strictly positive constants θ_1, θ_2 such that

$$\mu\left(\frac{\partial f}{\partial x_s}\right) + \frac{\theta_2}{\theta_1}\left\|\frac{\partial g}{\partial x_s}\right\| \qquad \text{and} \qquad \mu\left(\frac{\partial \mathrm{g}}{\partial \mathrm{z}}\right) + \frac{\theta_1}{\theta_2}\left\|\frac{\partial \mathrm{f}}{\partial \mathrm{z}}\right\| \tag{25}$$

are both uniformly negative definite.

Now, $\mu\left(\frac{\partial f}{\partial x_s}\right)$ and $\mu\left(\frac{\partial g}{\partial z}\right)$ are both uniformly negative by hypotheses. Furthermore, $\mu\left(\frac{\partial f}{\partial x_s}\right)$ tends to $-\infty$ as N increases: since $\left\|\frac{\partial f}{\partial z}\right\|$ and $\left\|\frac{\partial g}{\partial x_s}\right\|$ are bounded, this implies that there exists some N^* such that for any $N \geq N^*$ the two conditions in (25) are satisfied. □

Also, assume that actually the dynamics f and g do not depend explicitly on time. Then, under the conditions of the above Theorem, the reduced system is both contracting and autonomous, and so it tends towards a unique equilibrium point [43]. Thus, the original system converges to a unique equilibrium, where all x_i's are equal.

In addition, note that when the synchronization rate and the contraction rate of the reduced system both increase with N, this also increases robustness [41] to variability and disturbances.

C. How synchronization protects from noise

In this Section, we discuss briefly how the synchronization mechanism provided by dynamical quorum sensing protects from noise and variability in a fashion similar to the static mechanism studied in [21]. We show that the results of [21], to which the reader is referred for details about stochastic tools, extend straightforwardly to the case where the dynamics of the quorum variables cannot be neglected or indeed may play a central part, as studied in this paper.

Assume that the dynamics of each network element x_i in (22) is subject to noise, and consider, similarly to [21], the corresponding system of individual elements in Ito form

$$dx_i = \left(f(x_i, t) + kN(z - x_i)\right) dt + \sigma dW_i \qquad i = 1 \ldots N \tag{26}$$

where the all-to-all coupling in [21] has been replaced by a more general quorum sensing mechanism. The subsystems are driven by independent noise processes, and for simplicity the noise intensity σ in the equations above is assumed to be constant. We make no assumptions about noise acting directly on the dynamics of the environment/quorum vector z.

Proceeding exactly as in [21] yields similar results on the effect of noise. In particular, let $x^\bullet$ be the center of mass of the x_i, that is

$$x^\bullet = \frac{1}{N}\sum_i x_i$$

Notice that when all the nodes are synchronized onto some common solution, say $x_s(t)$, then, by definition, $x^\bullet = x_s(t)$.

Adding up the dynamics in (26) gives

$$dx^\bullet = \frac{1}{N}\left(\sum_i f(x_i,t)\right)dt + kN(z-x^\bullet)dt + \frac{1}{N}\sum_i \sigma dW_i \tag{27}$$

Let

$$\epsilon = f(x^\bullet,t) - \frac{1}{N}\left(\sum_{i=1}^N f(x_i,t)\right)$$

Note that $\epsilon = 0$ when all the nodes are synchronized.

By analogy with (26), equation (27) can then be written

$$dx^\bullet = \left(f(x^\bullet,t) + kN(z-x^\bullet) + \epsilon\right)dt + \frac{1}{N}\sum_i \sigma dW_i \tag{28}$$

Using the Taylor formula with integral remainder exactly as in [21] yields a bound on the distortion term ϵ, as a function of the nonlinearity, the coupling gain k, and the number of cells N,

$$\mathbb{E}(\|\epsilon\|) \;\leq\; \lambda_{\max}\left(\frac{\partial^2 f}{\partial x^2}\right)\quad \rho(kN)$$

where $\lambda_{\max}(\frac{\partial^2 f}{\partial x^2})$ is a uniform upper bound on the spectral radius of the Hessian $\frac{\partial^2 f}{\partial x^2}$, and $\rho(kN) \to 0$ as $kN \to +\infty$. In particular, in (28), both the distortion term ϵ and the average noise term $\frac{1}{N}\sum_i \sigma dW_i$ tend to zero as $N \to +\infty$.

Note that an additional source of noise may be provided by the environment on the quorum variables themselves. We made no assumptions above about such noise, which acts directly on the dynamics of the environment/quorum vector z. How it specifically affects the common quantity z in (26) could be further studied.

Finally, note that this noise protection property, combined with quorum sensing's computational advantage (alluded to in the introduction, see [21]) of achieving all-to-all coupling using only $2N$ connections instead of N^2 connections, may have interesting implications in terms of the recent results of [60], which show that standard deviation from nominal trajectories due to noise varies as the quartic root of the number of signalling events.

Similar results hold for the effects of bounded disturbances and dynamic variations.

VI. EXAMPLES

A. Synchronization of FitzHugh-Nagumo oscillators

To illustrate synchronization and population effects similar to those described in Section V A, consider a network of FitzHugh-Nagumo oscillators coupled through a dynamic medium,

$$\begin{aligned}
\dot{v}_i &= c\left(v_i + w_i - 1/3 v_i^3 + I\right) + kN\left(z - v_i\right)\\
\dot{w} &= -1/c\left(v_i - a + b w_i\right)\\
\dot{z} &= \tfrac{D_e}{N}\textstyle\sum_{i=1}^N (v_i - z) - d_e z
\end{aligned} \tag{29}$$

In what follows, system parameters are set as $a = 0.3$, $b = 0.2$, $c = 20$, $k = 1$, $d_e = D_e = 1$. Similarly to the proof of Theorem 9, consider the virtual system

$$\begin{aligned}
\dot{y}_1 &= c\left(y_1 + y_2 - 1/3 y_2^3 + I\right) + kN\left(z - y_1\right)\\
\dot{y}_2 &= -1/c\left(y_1 - a + b y_2\right)
\end{aligned}$$

whose Jacobian matrix is

$$J := \begin{bmatrix} c\left(1-y_1^2\right)-kN & c \\ -\frac{1}{c} & -\frac{b}{c} \end{bmatrix}$$

Using the matrix measure $\mu_{2,\Theta}$, with

$$\Theta = \begin{bmatrix} 1 & 0 \\ 0 & c \end{bmatrix}$$

yields $\mu_{2,\Theta}(J) = \mu_2(F)$, where

$$F = \Theta J \Theta^{-1} = \begin{bmatrix} c\left(1-y_1^2\right)-kN & 1 \\ -1 & -\frac{b}{c} \end{bmatrix}$$

Thus, the virtual system is contracting if the maximum eigenvalue of the symmetric part of F is uniformly negative. Similarly to Theorem 9, this is obtained if

$$N > \frac{c}{k} \tag{30}$$

That is, a sufficient condition for the virtual system to be contracting, and hence for network (29) to fulfill synchronization, is given by (30). Figures 4 and 5 illustrate the corresponding system behavior for values of N below and above this threshold.

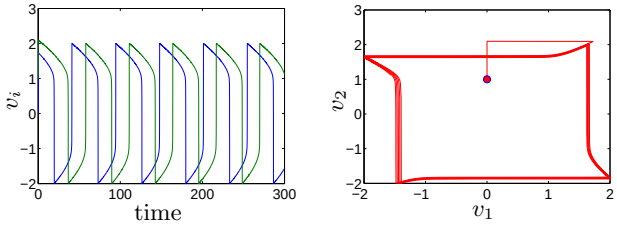

FIG. 4. (Color online) Simulation of network (29) for $N = 2$, showing the absence of synchronization. Left: time behavior of v_1, v_2. Right: network phase plot, with initial conditions denoted with a round marker.

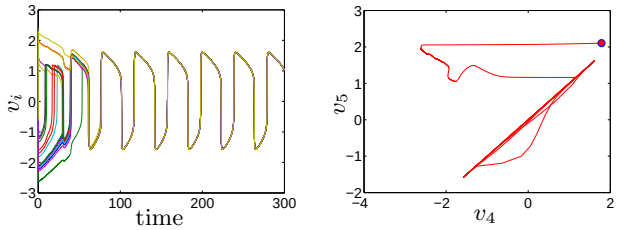

FIG. 5. (Color online) Simulation of network (29) for $N = 20$, showing synchronization.

B. Controlling synchronization of genetic oscillators

In Section IV we showed that bilateral coupling with the environment also allowed the synchronized behavior of the network nodes to be of a given period, by driving the environment variable by an exogenous signal having that period. Here we illustrate this result on a model of a population of genetic oscillators coupled by means of the concentration of a protein in the environment.

1. Genetic oscillators

Specifically, we consider the genetic circuit analyzed in [61] (a variant of [62]), and schematically represented in Figure 6. Such a circuit is composed of two engineered gene networks that have been experimentally implemented in *E. coli*; namely: the toggle switch [63] and an intercell communication system [2]. The toggle switch is composed of two transcription factors: the *lac* repressor, encoded by gene *lacI*, and the temperature-sensitive variant of the λcI repressor, encoded by the gene *cI857*. The expressions of *cI857* and *lacI* are controlled by the promoters P_{trc} and P_{L^*} respectively (for further details see [61]). The intercell communication system makes use of components of the quorum-sensing system from *Vibro fischeri* (see e.g. [16] and references therein). Such a mechanism allows cells to sense population density through the transcription factor LuxR, which is an activator of the genes expressed by the P_{lux} promoter, when a small molecule AI binds to it. This small molecule, synthesized by the protein LuxI, is termed as autoinducer and it can diffuse across the cell membrane.

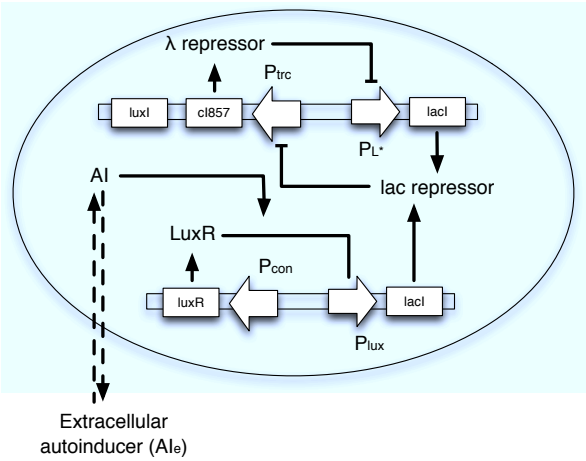

FIG. 6. A schematic representation of the genetic circuit: detailed circuit.

In [61], the following dimensionless simplified model is analyzed (see Figure 7):

$$\dot{u}_i = \frac{\alpha_1}{1+v_i^\beta} + \frac{\alpha_3 w_i^\eta}{1+w_i^\eta} - d_1 u_i \tag{31a}$$

$$\dot{v}_i = \frac{\alpha_2}{1+u_i^\gamma} - d_2 v_i \tag{31b}$$

$$\dot{w}_i = \varepsilon\left(\frac{\alpha_4}{1+u_i^\gamma} - d_3 w_i\right) + 2d\,(w_e - w_i) \tag{31c}$$

$$\dot{w}_e = \frac{D_e}{N}\sum_{i=1}^{N}(w_i - w_e) - d_e w_e \tag{31d}$$

where u_i, v_i and w_i denotes the (dimensionless) concentrations of the *lac* repressor, λ repressor and LuxR-AI activator respectively. The state variable w_e denotes instead the (dimensionless) concentration of the extracellular autoinducer.

In [61], a bifurcation analysis is performed for the above model, showing that synchronization can be attained for some range of the biochemical parameters of the circuit. However, as the objective of that paper was to analyze the onset of synchronization, the problem of guaranteeing a desired oscillatory behavior was not addressed. In what follows, using the results derived in the previous sections, we address the open problem of guaranteeing a desired period for the final oscillatory behavior of network (31).

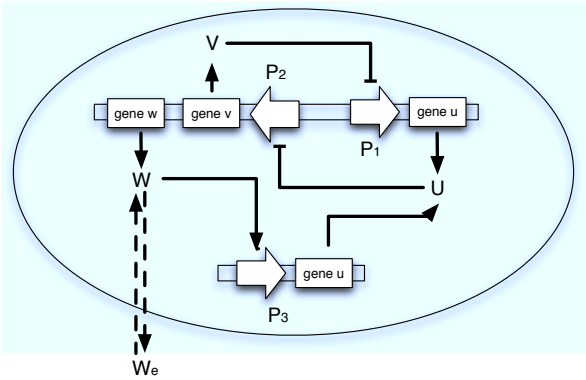

FIG. 7. Simplified circuit using for deriving the mathematical model (31). Both the promoters and transcription factors are renamed.

The control mechanism that we use here is an exogenous signal acting on the extracellular autoinducer concentration, see also [58]. That is, the idea is to modify (31d) as follows

$$\dot{w}_e = \frac{D_e}{N}\sum_{i=1}^{N}\left(w_i - w_e\right) - d_e w_e + r\left(t\right) \tag{32}$$

where $r\left(t\right)$ is some T-periodic signal. In the set up that we have in mind here, multiple copies of the genetic circuit of interest share the same surrounding solution, on which $r\left(t\right)$ acts. From the technological viewpoint, $r\left(t\right)$ can be implemented by controlling the temperature of the surrounding solution, and/or using e.g. the recently developed microfluidics technology (see e.g. [64] and references therein).

In what follows, we will use Theorem 4 to find a set of biochemical parameters that ensure synchronization of (31a)-(31d). This, using the results of Section IV, immediately implies that the forced network (31a)-(31c), (32) globally exponentially converges towards a T-periodic final behavior.

System (31) has the same structure as (9), with $x_i = \left[u_i, v_i, w_i\right]^T$, $z = w_e$, and:

$$\begin{aligned}
f\left(x_i,t\right) &= \begin{bmatrix} \frac{\alpha_1}{1+v_i^\beta} + \frac{\alpha_3 w_i^\eta}{1+w_i^\eta} - d_1 u_i \\ \frac{\alpha_2}{1+u_i^\gamma} - d_2 v_i \\ \varepsilon\left(\frac{\alpha_4}{1+u_i^\gamma} - d_3 w_i\right) \end{bmatrix} \\
k_z\left(z\right) - k_x\left(x_i\right) &= \begin{bmatrix} 0 \\ 0 \\ 2d\left(w_e - w_i\right) \end{bmatrix} \\
g\left(z,t\right) &= -d_e w_e \\
\textstyle\sum_{i=1}^{N}\left[u_x\left(x_i\right) - u_z\left(z\right)\right] &= \frac{D_e}{N}\textstyle\sum_{i=1}^{N}\left(w_i - w_e\right)
\end{aligned}$$

We know from Theorem 7 that all nodes trajectories converge towards each other if the reduced order system

$$\begin{aligned}
\dot{u}_c &= \tfrac{\alpha_1}{1+v_c^\beta} + \tfrac{\alpha_3 w_c^\eta}{1+w_c^\eta} - d_1 u_c \\
\dot{v}_c &= \tfrac{\alpha_2}{1+u_c^\gamma} - d_2 v_c \\
\dot{w}_c &= \varepsilon\left(\tfrac{\alpha_4}{1+u_c^\gamma} - d_3 w_c\right) + 2d\left(w_e - w_c\right) \\
\dot{w}_e &= \tfrac{D_e}{N}\textstyle\sum_{i=1}^{N}\left(w_c - w_e\right) - d_e w_e
\end{aligned}$$

is contracting. In turn, this is ensured if the following conditions are fulfilled:

1. $f\left(x_i,t\right) - k_x\left(x_i\right)$ is contracting;
2. $g\left(z,t\right) - N u_z\left(z\right)$ is contracting.

Indeed, in this case the conditions in (20) are fulfilled. That is, contraction is ensured if there exist some matrix measures, μ_* and μ_{**}, such that

$$\mu_* \left((x_i, t) - k_x (x_i) \right) \quad \text{and} \quad \mu_{**} \left(g(z,t) - N u_z (z) \right)$$

are uniformly negative definite. We use the above two conditions in order to obtain a set of biochemical parameters ensuring node convergence. A possible choice for the above matrix measures is $\mu_* = \mu_{**} = \mu_1$ (see [65], [58]). Clearly, other choices for the matrix measures μ_* and μ_{**} can be made, leading to different algebraic conditions, and thus to (eventually) a different choice of biochemical parameters.

We assume that $\beta = \eta = \gamma = 2$, and show how to find a set of biochemical parameters satisfying the above two conditions.

Condition 1. Differentiation of $\frac{\partial f}{\partial x_i} - \frac{\partial k}{\partial x_i}$ yields the Jacobian matrix (where the subscripts have been omitted)

$$J_i := \begin{bmatrix} -d_1 & \frac{-2\alpha_1 v}{(1+v^2)^2} & \frac{2\alpha_3 w}{(1+w^2)^2} \\ \frac{-2\alpha_2 u}{(1+u^2)^2} & -d_2 & 0 \\ \frac{-2\varepsilon\alpha_4 u}{(1+u^2)^2} & 0 & -\varepsilon d_3 - 2d \end{bmatrix} \tag{33}$$

Now, by definition of μ_1, we have:

$$\mu_1 (J_i) = \max \Big\{ -d_1 + \tfrac{2\alpha_2 u}{(1+u^2)^2} + \tfrac{2\varepsilon\alpha_4 u}{(1+u^2)^2}, \\ -d_2 + \tfrac{2\alpha_1 v}{(1+v^2)^2}, -\varepsilon d_3 - 2d + \tfrac{2\alpha_3 w}{(1+w^2)^2} \Big\}$$

Thus, J_i is contracting if $\mu_1 (J_i)$ is uniformly negative definite. That is,

$$\begin{aligned} &-d_1 + \tfrac{2\alpha_2 u}{(1+u^2)^2} + \tfrac{2\varepsilon\alpha_4 u}{(1+u^2)^2} < 0 \\ &-d_2 + \tfrac{2\alpha_1 v}{(1+v^2)^2} < 0 \\ &-\varepsilon d_3 - 2d + \tfrac{2\alpha_3 w}{(1+w^2)^2} < 0 \end{aligned} \tag{34}$$

uniformly. Notice now that the maximum of the function $a(v) = \frac{\bar{a} v}{(1+v^2)^2}$ is $\hat{a} = \frac{3\sqrt{3}\bar{a}}{16}$. Thus, the set of inequalities (34) is fulfilled if:

$$\begin{aligned} &-d_1 + \tfrac{6\alpha_2\sqrt{3}}{16} + \tfrac{6\varepsilon\alpha_4\sqrt{3}}{16} < 0 \\ &-d_2 + \tfrac{6\alpha_1\sqrt{3}}{16} < 0 \\ &-\varepsilon d_3 - 2d + \tfrac{6\alpha_3\sqrt{3}}{16} < 0 \end{aligned} \tag{35}$$

uniformly.

Condition 2 In this case it is easy to check that the matrix $J_e := \frac{\partial g}{\partial z} - N\frac{\partial u}{\partial z}$ is contracting for any choice of the (positive) biochemical parameters D_e, d_e.

Thus, we can conclude that any choice of biochemical parameters fulfilling (35) ensures synchronization of the network onto a periodic orbit of period T. In [61], it was shown that a set of parameters for which synchronization is attained is: $\alpha_1 = 3$, $\alpha_2 = 4.5$, $\alpha_3 = 1$, $\alpha_4 = 4$, $\varepsilon = 0.01$, $d = 2$, $d_1 = d_2 = d_3 = 1$. We now use the guidelines provided by (35) to make a minimal change of the parameters values ensuring network synchronization with oscillations of period T. Specifically, such conditions can be satisfied by setting $d_1 = 6$, $d_2 = 2$. Figure 8 shows the behavior of the network for such a choice of the parameters. Finally, Figure 9 shows a simulation of the network (with $N = 2$) when the biochemical parameters are chosen so as to violate the two conditions above. In such a figure, both the time behavior of w_i and phase plot are shown, indicating that synchronization is indeed not attained.

Note again that, depending on actual parameter values, the overall system may or not be contracting, and therefore synchronization to a common period is the result of coordination through the shared variable and not just of the theorem on periodic inputs of Section II A.

2. Communication over different media

In the above Section, we assumed that all the genetic circuits shared the same surrounding solution. We now analyze the case where two different groups of genetic circuits are surrounded by two different media. The communication between groups is then left to some (possibly artificial) communication strategy between the two media.

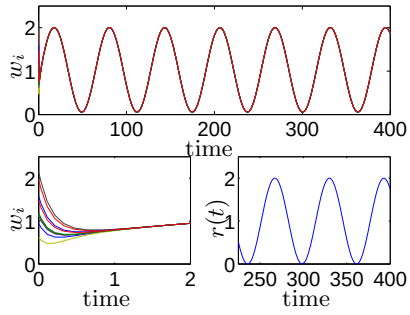

FIG. 8. (Color online) Behavior of (31a)-(31c), (32), when $N = 10$ and $r(t) = 1 + \sin(0.1t)$. Notice that the nodes have initial different conditions, and that they all converge (at approximatively $t = 2$) onto a common asymptotic having the same period as $r(t)$.

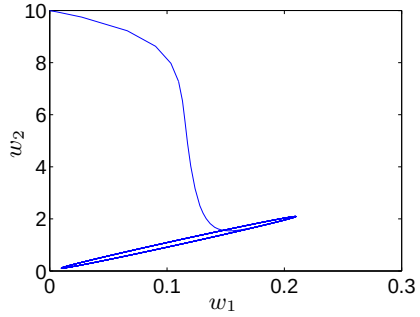

FIG. 9. (Color online) Behavior of (31a)-(31c), (32), when $N = 2$ and all the α's are increased, violating condition 1 and condition 2. The phase plot shows that synchronization is not attained: w_1 is on the x-axis, w_2 is on the y-axis.

We now assume that only one of the two media is forced by the exogenous T-periodic signal $r(t)$, while the two media communicate with each other in a diffusive way. The mathematical model that we analyze here is then:

$$\begin{aligned}
\dot{u}_{i1} &= \tfrac{\alpha_1}{1+v_{i1}^{\beta}} + \tfrac{\alpha_3 w_{i1}^{\eta}}{1+w_{i1}^{\eta}} - d_1 u_{i1} \\
\dot{v}_{i1} &= \tfrac{\alpha_2}{1+u_{i1}^{\gamma}} - d_2 v_{i1} \\
\dot{w}_{i1} &= \varepsilon\left(\tfrac{\alpha_4}{1+u_{i1}^{\gamma}} - d_3 w_{i1}\right) + 2d(w_{e1} - w_{i1}) \\
\dot{w}_{e1} &= \tfrac{D_e}{N}\textstyle\sum_{i=1}^{N}(w_{i1} - w_{e1}) - d_e w_{e1} + r(t) + \phi(w_{e2}) - \phi(w_{e1}) \\
\dot{u}_{i2} &= \tfrac{\bar{\alpha}_1}{1+v_{i2}^{\beta}} + \tfrac{\bar{\alpha}_3 w_{i2}^{\eta}}{1+w_{i2}^{\eta}} - \bar{d}_1 u_{i2} \\
\dot{v}_{i2} &= \tfrac{\bar{\alpha}_2}{1+u_{i2}^{\gamma}} - \bar{d}_2 v_{i2} \\
\dot{w}_{i2} &= \varepsilon\left(\tfrac{\bar{\alpha}_4}{1+u_{i2}^{\gamma}} - d_3 w_{i2}\right) + 2d(w_{e2} - w_{i2}) \\
\dot{w}_{e2} &= \tfrac{\bar{D}_e}{N}\textstyle\sum_{i=1}^{N}(w_{i2} - w_{e2}) - \bar{d}_e w_{e2} + \phi(w_{e1}) - \phi(w_{e2})
\end{aligned} \tag{36}$$

where $x_{i1} = [u_{i1}, v_{i1}, w_{i1}]^T$ and $x_{i2} = [u_{i2}, v_{i2}, w_{i2}]^T$ denote the set of state variables of the i-th oscillator of the first and second group respectively. Analogously, w_{e1} and w_{e2} denote the extracellular autoinducer concentration surrounding the first and second group of genetic circuits.

Notice that the biochemical parameters of the nodes composing the two groups and of their corresponding media are not identical. Specifically, for the first group we use the same parameters as in the previous section, while for the second group we use parameters which differ from parameters of the first group by approximatively 50% (so as to still satisfy the two conditions of the previous Section). To ensure concurrent synchronization, we design the coupling function between the media ($\phi(\cdot)$) by using the guidelines provided by Theorem 6. Furthermore, using Theorem 8 we can conclude that the final behavior of the two groups is T-periodic.

It is straightforward to check that the hypotheses of Theorem 6 are all satisfied if:

- the biochemical parameters of the two groups fulfill the conditions in (35);

- the coupling function $\phi(\cdot)$ is increasing.

In fact, the topology of the autonomous level of the network is input equivalent by construction. Figure 10 shows the behavior of (36) when the biochemical parameters of the oscillators are tuned as in the previous Section, and $\phi(x) = Kx$, with $K = 0.1$.

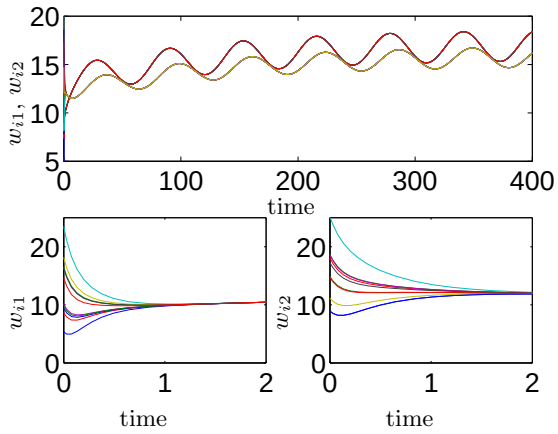

FIG. 10. (Color online) Behavior of (36) when $r(t) = 1 + \sin(0.1t)$. Both groups consists of $N = 10$ nodes. Concurrent synchronization is attained for the network. The time behavior of the first group of nodes is in red (upper line), while the time behavior of the second group is in yellow (lower line). Both the groups exhibit a final, synchronized, behavior having the same period as $r(t)$.

3. Co-existence of multiple node dynamics

We now consider the case where the two groups analyzed above are identical, but connected with each other by means of a third group composed of Van der Pol oscillators. For such oscillators, the coupling between elements of the same goup is also implemented by means of a quorum-sensing mechanism. Communication between the three groups occurs by means of some coupling between their media. The mathematical model considered here is then:

$$
\begin{aligned}
\dot{u}_{i1} &= \tfrac{\alpha_1}{1+v_{i1}^{\beta}} + \tfrac{\alpha_3 w_{i1}^{\eta}}{1+w_{i1}^{\eta}} - d_1 u_{i1} \\
\dot{v}_{i1} &= \tfrac{\alpha_2}{1+u_{i1}^{\gamma}} - d_2 v_{i1} \\
\dot{w}_{i1} &= \varepsilon\left(\tfrac{\alpha_4}{1+u_{i1}^{\gamma}} - d_3 w_{i1}\right) + 2d(w_{e1} - w_{i1}) \\
\dot{w}_{e1} &= \tfrac{D_e}{N}\textstyle\sum_{i=1}^{N}(w_{i1} - w_{e1}) - d_e w_{e1} + \phi(w_{e3}) - \phi(w_{e1}) \\
\dot{u}_{i2} &= \tfrac{\alpha_1}{1+v_{i2}^{\beta}} + \tfrac{\alpha_3 w_{i2}^{\eta}}{1+w_{i2}^{\eta}} - d_1 u_{i2} \\
\dot{v}_{i2} &= \tfrac{\alpha_2}{1+u_{i2}^{\gamma}} - d_2 v_{i2} \\
\dot{w}_{i2} &= \varepsilon\left(\tfrac{\alpha_4}{1+u_{i2}^{\gamma}} - d_3 w_{i2}\right) + 2d(w_{e2} - w_{i2}) \\
\dot{w}_{e2} &= \tfrac{D_e}{N}\textstyle\sum_{i=1}^{N}(w_{i2} - w_{e2}) - d_e w_{e2} + \phi(w_{e3}) - \phi(w_{e2}) \\
\dot{y}_{1i} &= y_{2i} \\
\dot{y}_{2i} &= -\alpha\left(y_{1i}^2 - \beta\right) y_{2i} - \omega^2 y_{1i} + K(w_{e3} - y_{1i}) \\
\dot{w}_{e3} &= \tfrac{K}{N_{vdp}}\textstyle\sum_{i=1}^{N}(y_{2i} - w_{e3}) + g(w_{e3}) + \phi(w_{e1}) + \phi(w_{e2}) - 2\phi(w_{e3})
\end{aligned}
\tag{37}
$$

with $[y_{1i}, y_{2i}]^T$ denoting the state variables of the i-th Van der Pol oscillator, and with N_{vdp} indicating the number of Van der Pol oscillators in the network. In the above model the Van der Pol oscillators are coupled by means of the medium $w_{e3} \in \mathbb{R}$. The three media, i.e. w_{e1}, w_{e2}, w_{e3}, communicate by means of the coupling function $\phi(\cdot)$, assumed to be linear. We assume that the function g governing the intrinsic dynamics of the medium w_{e3} is smooth with bounded derivative. The parameters for the Van der Pol oscillator are set as follows: $\alpha = \beta = \omega = 1$. Notice that now no external inputs is applied on the network.

Recall that Theorem 6 ensures synchronization under the following conditions:

1. contraction of each group composing the network;

2. topology of the autonomous level of the network connected and input equivalent.

Notice that the second condition is satisfied for the network of our interest. Furthermore, contraction of the two groups composed of genetic oscillators is ensured if the their biochemical parameters satisfy the inequalities in (35).

To guarantee the convergent behavior of the group composed of Van der Pol oscillators, we have to check that there exist two matrix measures, μ_* and μ_{**}, showing contraction of the following two matrices:

$$J_1 = \begin{bmatrix} 0 & 1 \\ -\alpha\left(y_{2i}^2 - \beta\right) - \omega^2 & -2\alpha y_{2i} y_{1i} - K \end{bmatrix} \tag{38a}$$

$$J_2 = \frac{\partial g}{\partial w_{e3}} - K \tag{38b}$$

Now in [49], using the Euclidean matrix measure μ_2, it is shown that the matrix (38a) is contracting if $K > \alpha$. On the other hand, to ensure contraction of J_2, we have to choose $K > \bar{G}$, where $\bar{G}$ is the maximum of $\frac{\partial g}{\partial w_{e3}}$. Thus, contraction of the group composed of Van der Pol oscillators is guaranteed if the coupling gain, K, is chosen such that:

$$K > \max\left\{\alpha, \bar{G}\right\}$$

Using $g(x) = \sin(x)$, $K = 2.5$, $N_{vdp} = 2$ and $\phi(x) = Kx$, with $K = 3$, Figure 11 shows that all the nodes of the two groups of genetic oscillators in (37) are synchronized, in agreement with the theoretical analysis. Figure 12 also shows that the two nodes belonging to the group of Van der Pol oscillators are synchronized with each other.

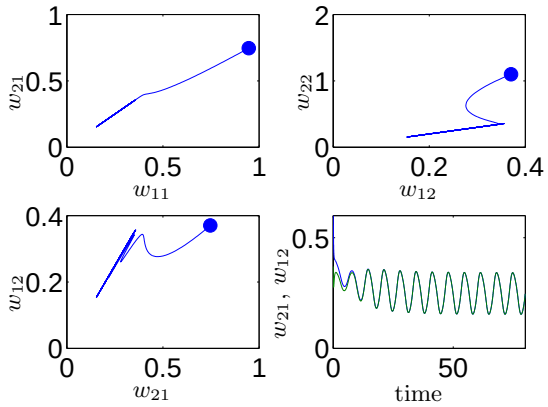

FIG. 11. (Color online) Behavior of (37): each of the two groups of genetic oscillators contains $N = 4$ nodes. Top: phase plot of the nodes belonging to the first group of genetic oscillators (left) and phase plot of the nodes belonging to the second group of genetic oscillators (right). Bottom: phase plot of two nodes belonging to the two different groups of genetic oscillators (left) and their time behavior. Both the phase plots and the time series show that synchronization is attained.

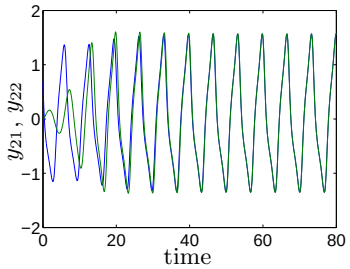

FIG. 12. (Color online) Time behavior of the two nodes composing the group of Van der Pol oscillators in (37).

C. Analysis of a general Quorum-Sensing pathway

In the previous Section, we showed that our results (with appropriate choice of matrix measure) can be used to derive easily verifiable conditions on the biochemical parameters of the genetic oscillator ensuring contraction, and hence synchronization (onto a periodic orbit of desired period) and concurrent synchronization. We now show that our methodology can be applied to analyze a wide class of biochemical systems involved in cell-to-cell communication.

We focus on the analysis of the pathway of the quorum sensing mechanism that uses as autoinducers, molecules from the AHL (acyl homoserine lactone) family. The quorum sensing pathway implemented by AHL (see Figure 13) is one of the most common for bacteria and drives many transcriptional systems regulating their basic activities.

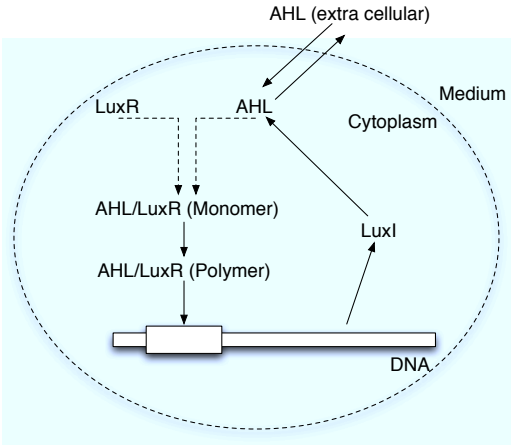

FIG. 13. The quorum sensing pathway implemented by AHL

We now briefly describe the pathway of our interest (see [66] for further details). The enzyme LuxI produces AHL at (approximately) a constant rate. AHL in turn diffuses into and out of the cell and forms (in the cytoplasm) a complex with the receptor LuxR. Such complex polymerizes and then acts as a transcription factor, by binding the DNA. This causes the increase of the production of LuxI, generating a positive feedback loop.

The pathway can be described by a set of ordinary differential equations (using the law of mass action, see [67], [66]). Specifically, denoting with x_e the mass of AHL outside of the cell and with x_c the mass of AHL within the cell, we have the following mathematical model:

$$\begin{aligned} \dot{x}_c &= \alpha + \tfrac{\beta x_c^n}{x_{thresh}^n + x_c^n} - \gamma_c x_c - d_1 x_c - d_2 x_e \\ \dot{x}_e &= d_1 x_c - d_2 x_e - \gamma_e x_e \end{aligned} \tag{39}$$

The physical meaning of the parameters in (39) is given in Table II.

TABLE II. Biochemical parameters for system (39)

Parameter	physical meaning
α	Low production rate of AHL
β	Increase of production rate of AHL
γ_c	Degradation rate of AHL in the cytosol
γ_e	Degradation rate of AHL outside the cell
d_1	Diffusion rate of the extracellular AHL
d_2	Diffusion of the intracellular AHL
x_{thresh}	Threshold of AHL between low and increased activity
n	Degree of polymerization

Now, contraction of the above system is guaranteed if

1. $-\gamma_c + \frac{2\beta x_{thresh}^2 x_c}{\left(x_{thresh}^2+x_c^2\right)^2}$ is uniformly negative definite;

2. $-d_2 - \gamma_e$ is uniformly negative definite.

Recall that x_c and x_e are both scalars. Now, the second condition is satisfied since system parameters are all positive. That is, to prove contraction we have only to guarantee that

$$-\gamma_c + \frac{2\beta x_{thresh}^2 x_c}{\left(x_{thresh}^2 + x_c^2\right)^2}$$

is uniformly negative. Since

$$-\gamma_c + \frac{2\beta x_{thresh}^2 x_c}{\left(x_{thresh}^2 + x_c^2\right)^2} \leq -\gamma_c + \frac{3\beta\sqrt{3}}{8x_{thresh}}$$

contraction is ensured if the biochemical parameters β, g and x_{thresh} fulfill the following condition

$$\frac{\beta}{x_{thresh}} < \frac{8\gamma_c}{3\sqrt{3}}$$

VII. CONCLUDING REMARKS

In this paper, we presented a systematic methodology to derive conditions for the global exponential convergence of biochemical models modeling quorum sensing systems. To illustrate the effectiveness of our results and to emphasize the use of our techniques in synthetic biology design, we analyzed a set of biochemical networks where the quorum sensing mechanism is involved as well as a typical pathway of the quorum sensing. In all such cases we showed that our results can be used to determine system parameters and dynamics ensuring convergence.

Appendix A: Proofs

To prove Theorem 3 we need the following Lemma, which is a generalization of a result proven in [58]:

Lemma 1. *Consider the block- partition for a square matrix J:*

$$J = \begin{bmatrix} A(x) & B(x,y) \\ C(x,y) & D(y) \end{bmatrix}$$

where A and D are square matrices of dimensions $n_A \times n_A$ and $n_D \times n_D$ respectively. Assume that A and B are contracting with respect to μ_A and μ_D (induced by the vector norm $|\bullet|_A$ and $|\bullet|_D$). Then, J is contracting if there exists two positive real numbers θ_1, θ_2 such that

$$\mu_A(A) + \tfrac{\theta_2}{\theta_1} \|C(x,y)\|_{A,D} \leq -c_A^2$$
$$\mu_D(D) + \tfrac{\theta_1}{\theta_2} \|B(x,y)\|_{D,A} \leq -c_B^2$$

where $\|\bullet\|_{A,D}$ and $\|\bullet\|_{D,A}$ are the operator norms induced by $|\bullet|_A$ and $|\bullet|_D$ on the linear operators C and B. Furthermore, the contraction rate is $c^2 = \max\left\{c_A^2, c_B^2\right\}$.

Proof. Let $z := (x,y)^T$. We will show that, with the above hypotheses, J is contracting with respect to the matrix measure induced by the following vector norm:

$$|z| := \theta_1 |x|_A + \theta_2 |y|_D$$

with $\theta_1, \theta_2 > 0$. In this norm, we have

$$|(I+hJ)z| = \theta_1 |(I+hA)x + hBy|_A + \theta_2 |(I+hD)y + hCx|_D$$

Thus,

$$|(I+hJ)z| \leq \theta_1 |(I+hA)x|_A + h\theta_1 |By|_{D,A} + \\ +\theta_2 |(I+hD)y|_D + h\theta_2 |Cx|_{A,D}$$

Pick now $h > 0$ and a unit vector z (depending on h) such that $\|(I+hJ)z\| = |(I+hJ)z|$. We have, dropping the subscripts for the norms:

$$\tfrac{1}{h}(\|I+hJ\|-1) \leq \tfrac{1}{h}\left(\|I+hA\|-1+\tfrac{\theta_2}{\theta_1}h\|C\|\right)|x|\,\theta_1 + \\ +\tfrac{1}{h}\left(\|I+hD\|-1+\tfrac{\theta_1}{\theta_2}h\|B\|\right)|y|\,\theta_2$$

Since $1 = |z| = \theta_1 |x|_A + \theta_2 |y|_B$, we finally have

$$\tfrac{1}{h}(\|I+hJ\|-1) \leq \max\left\{\tfrac{1}{h}\left(\|I+hA\|-1+\tfrac{\theta_2}{\theta_1}h\|C\|\right), \\ \tfrac{1}{h}\left(\|I+hD\|-1+\tfrac{\theta_1}{\theta_2}h\|B\|\right)\right\}$$

Taking now the limit for $h \to 0^+$:

$$\mu(J) \leq \max\left\{\mu(A)_A + \frac{\theta_2}{\theta_1}\|C\|, \mu(D)_D + \frac{\theta_1}{\theta_2}\|B\|\right\}$$

thus proving the result. □

Following the same arguments, Lemma 1 can be straightforwardly extended to the case of a real matrix J partitioned as

$$J = \begin{bmatrix} J_{11} & J_{12} & \dots & J_{1N} \\ \dots & \dots & \dots & \dots \\ J_{N1} & J_{N2} & \dots & J_{NN} \end{bmatrix}$$

where the diagonal blocks of J are all square matrices. Then J is contracting if

$$\begin{aligned} &\mu(J_{11}) + \tfrac{\theta_2}{\theta_1}\|J_{12}\| + \ldots + \tfrac{\theta_N}{\theta_1}\|J_{1N}\| \leq -c_{11}^2 \\ &\dots \\ &\mu(J_{NN}) + \tfrac{\theta_1}{\theta_N}\|J_{N1}\| + \ldots + \tfrac{\theta_{N-1}}{\theta_N}\|J_{1N}\| \leq -c_{NN}^2 \end{aligned} \tag{A1}$$

(where subscripts for matrix measures and norms have been neglected).

Proof of Theorem 3

The assumption of input equivalence for the nodes implies the existence of a linear invariant subspace associated to the concurrent synchronization final behavior. We will prove convergence towards such a subspace, by proving that the network dynamics is contracting. Let μ_f be the matrix measure where the nodes dynamics is contracting and define: $X := (x_1^T, \ldots, x_N^T)^T$, $F(X)$ as the stack of all intrinsic nodes dynamics, $H(X)$ the stack of nodes coupling functions. We want to prove that there exist a matrix measure, μ, (which is in general different from μ_f) where the whole network dynamics is contracting. Denote with $L := \{l_{ij}\}$ the Laplacian matrix [68] of the network and define the matrix $\tilde{L}(X)$, whose ij-th block, $\tilde{L}_{ij}(X)$, is defined as follows:

$$\tilde{L}_{ij}(X) := l_{ij}\frac{\partial h_{\gamma(i)}}{\partial x_j}$$

(Notice that if all the nodes are identical and have the same dynamics and the same coupling functions, then $\tilde{L}$ can be written in terms of the Kronecker product, $\otimes$, as $(L \otimes I_n)\frac{\partial H}{\partial X}$, with n denoting the dimension of the nodes and I_n the $n \times n$ identity matrix.)

The Jacobian of (5) is then:

$$J := \left[\frac{\partial F}{\partial X} - \tilde{L}(X)\right] \tag{A2}$$

The system is contracting if

$$\mu\left(\frac{\partial F}{\partial X} - \tilde{L}(X)\right)$$

is uniformly negative definite. Now:

$$\mu\left(\frac{\partial F}{\partial X} - \tilde{L}(X)\right) \leq \mu\left(\frac{\partial F}{\partial X}\right) + \mu\left(-\tilde{L}(X)\right)$$

Notice that, by hypotheses, the matrix $-\tilde{L}(X)$ has negative diagonal blocks and zero column sum. Thus, using (A1) with $\theta_i = \theta_j$ for all $i, j = 1, \ldots, N$, $i \neq j$ yields

$$\mu\left(-\tilde{L}(X)\right) = 0$$

Thus:

$$\mu\left(\frac{\partial F}{\partial X} - \tilde{L}(X)\right) \leq \mu\left(\frac{\partial F}{\partial X}\right)$$

Since the matrix $\frac{\partial F}{\partial X}$ is block diagonal, i.e. all of its off-diagonal elements are zero, (A1) yields:

$$\mu\left(\frac{\partial F}{\partial X}\right) = \max_{x,t,i}\left\{\mu_f\left(\frac{\partial f_{\gamma(i)}}{\partial x}\right)\right\}$$

The theorem is then proved by noticing that by hypothesis the right hand side of the above expression is uniformly negative.

---

[1] S. Strogatz, *Sync: the emerging science of spontaneous order* (Hyperion (New York, USA), 2003).
[2] L. You, R. C. 3rd, R. Weiss, and F. Arnold, Nature, **428**, 868 (2004).
[3] D. McMillen, N. Kopell, J. Hasty, and J. Collins, Proceedings of the National Academy of Science, **99**, 679 (2002).
[4] S. Yagamuchi, H. Isejima, T. Matsuo, R. Okura, and K. Yagita, Science, **302**, 2531 (2003).
[5] E. Pye, Canadian Journal of Botany, **47**, 271 (1969).
[6] A. Winfree, *The geometry of biological time, 2nd Ed.* (Springer (New York), 2001).
[7] M. Newman, A. Barabasi, and D. Watts, *The structure and dynamics of complex networks* (Princeton University Press (Princeton, NJ, USA), 2006).
[8] D. Gonze, S. Bernard, C. Walterman, A. Kramer, and H. Herzerl, Biophyscal Journal, **89**, 120 (2005).
[9] J. J. Tyson, A. Csikasz-Nagy, and B. Novak, Bioessays, **24**, 1095 (2002).
[10] E. M. Izhikevich, *Dynamical Systems in Neuroscience: The Geometry of Excitability and Bursting* (MIT Press (Cambridge, MA, USA), 2006).
[11] M. A. Henson, Journal of Theoretical Biology, **231**, 443 (2004).
[12] E. Park, Z. Feng, and D. M. Durand, Biophysical Journal, **95**, 1126 (2008).
[13] A. Bohn and J. Gracia-Ojalvo, Journal of Theoretical Biology, **250**, 37 (2008).
[14] M. Miller and B. Bassler, Annual Review of Microbiology, **55**, 165 (2001).
[15] C. Nardelli, B. Bassler, and S. Levin, Journal of Biology, **7**, 27 (2008).
[16] W. Ng and B. Bassler, Annual Review of Genetics, **43**, 197 (2009).
[17] C. Anetzberger, T. Pirch, and K. Jung, Molecular Microbiology, **2**, 267 (2009).
[18] C. D. Nadell, J. Xavier, S. A. Levin, and K. R. Foster, PLoS Computational Biolody, **6**, e14 (2008).
[19] B. Pesaran, J. Pezaris, M. Sahani, P. Mitra, and R. Andersen, Nature, **5**, 805 (2002).
[20] S. E. Boustani, O. Marre, P. Behuret, P. Yger, T. Bal, A. Destexhe, and Y. Fregnac, PLoS Computational Biolody, **5**, e1000519 (2009).
[21] N. Tabareau, J. Slotine, and Q. Pham, PLoS Computational Biology, **6**, e1000637 (2010).
[22] C. Anastassiou, S. M. Montgomery, M. Barahona, G. Buzsaki, and C. Koch, The Journal of Neuroscience, **30**, 1925 (2010).

[23] M. Toiya, H. Gonzalez-Ochoa, V. K. Vanag, S. Fraden, and I. R. Epstein, The Journal of Physical Chemistry Letters, **1**, 1241 (2010).
[24] M. Toiya, V. K. Vanag, and I. R. Epstein, Angew. Chem. Int. Ed., **47**, 7753 (2008).
[25] F. Frohlich and D. A. McCormick, Neuron, **67**, 129 (2010).
[26] E. Mann and O. Paulsen, Neuron, **67**, 3 (2010).
[27] E. Kandel, J. Schwartz, and T. Jessel, *Principles of Neural Science (4th Edition)* (Oxforn University Press, 2000).
[28] E. Borenstein and S. Ullman, IEEE Transactions on Pattern Analysis and Machine Intelligence, **30**, 2109 (2008).
[29] D. George and J. Hawkins, PLoS Computational Biolody, **5**, e1000532 (2009).
[30] G. Gigante, M. Mattia, J. Braun, and P. DelGiudice, PLoS Computational Biolody, **5**, e1000430 (2009).
[31] G. Yu and J. Slotine, IEEE Transactions on Neural Networks, **20**, 1871 (2009).
[32] R. Toth, A. F. Taylor, and M. R. Tinsley, The Journal of Physical Chemistry, **110**, 10170 (2006).
[33] J. Javaloyes, M. Perrin, and A. Politi, Physical Review E, **78**, 011108 (2008).
[34] T. Gregor, K. Fujimoto, N. Masaki, and S. Sawai, Science, **328**, 1021 (2010).
[35] A. Prindle and J. Hasty, Science, **328**, 987 (2010).
[36] G. Katriel, Physica D, **237**, 2933 (2008).
[37] J. Zhang, Z. Yuan, and T. Zhou, Physical Review E, **79**, 041903 (2009).
[38] V. Resmi, G. Ambika, and R. E. Amritkar, Physical Review E, **81**, 046216 (2010).
[39] J. Garcia-Ojalvo, M. B. Elowitz, and S. H. Strogatz, Proc. of the Natl. Acad. of Sci., **101**, 10955 (2004).
[40] G. Russo and M. di Bernardo, Journal of Computational Biology, **16**, 379 (2009).
[41] Q. C. Pham and J. J. E. Slotine, Neural Networks, **20**, 62 (2007).
[42] E. Guirey, M. Bees, A. Martin, and M. Srokosz, Physical Review E, **81**, 051902 (2010).
[43] W. Lohmiller and J. J. E. Slotine, Automatica, **34**, 683 (1998).
[44] P. Hartman, Canadian Journal of Mathematics, **13**, 480 (1961).
[45] D. C. Lewis, American Journal of Mathematics, **71**, 294 (1949).
[46] A. Pavlov, A. Pogromvsky, N. van de Wouv, and H. Nijmeijer, Systems and Control Letters, **52**, 257 (2004).
[47] D. Angeli, IEEE Transactions on Automatic Control, **47**, 410 (2002).
[48] W. Lohmiller and J. J. Slotine, International Journal of Control, **78**, 678 (2005).
[49] W. Wang and J. J. E. Slotine, Biological Cybernetics, **92**, 38 (2005).
[50] G. Dahlquist, *Stability and error bounds in the numerical integration of ordinary differential equations* (Transanctions of the Royal Institute Technology (Stockholm), 1959).
[51] S. M. Lozinskii, Izv. Vtssh. Uchebn. Zaved Matematika, **5**, 222 (1959).
[52] J. Slotine, International Journal of Adaptive Control and Signal Processing, **17**, 397 (2003).
[53] M. Golubitsky, I. Stewart, and A. Torok, SIAM Journal on Applied Dynamical Systems, **4**, 78 (2005).
[54] G. Russo and M. di Bernardo, in *International Symposium on Circuits and Systems* (2009) pp. 305–308.
[55] S. Boccaletti, V. Latora, Y. Moreno, M. Chavez, and D. Hwang, Physics Report, **424**, 175 (2006).
[56] M. E. Newman, SIAM Review, **45**, 167 (2003).
[57] S. Chung, J. Slotine, and D. Miller, A.I.A.A. Journal of Guidance, Control and Dynamics, **30**, 390 (2007).
[58] G. Russo, M. di Bernardo, and E. D. Sontag, PLoS Computational Biolody, **6**, e1000739 (2010).
[59] Z. Szallasi, J. Stelling, and V. Periwal, *System Modeling in Cellular Biology: From Concepts to Nuts and Bolts* (The MIT Press, 2006).
[60] I. Lestas, G. Vinnicombe, and J. Paulsson, Nature, **467**, 174 (2010).
[61] A. Kuznetsov, M. Kaern, and N. Kopell, SIAM Journal of Applied Mathematics, **65**, 392 (2004).
[62] H. Kobayashi, M. Kaern, M. Araki, K. Chung, T. Gardner, C. Cantor, and J. Collins, Proceedings of the National Academy of Science, **101**, 8414 (2004).
[63] T. Gardner, C. Cantor, and J. Collins, Nature, **403**, 339 (2000).
[64] D. J. Beebe, G. Mensing, and G. Walker, Annual Reviews of Biomedical Engineering, **4**, 261 (2002).
[65] G. Russo, M. di Bernardo, and J. Slotine, "A graphical algorithm to prove contraction of nonlinear circuits and systems," (2010), iEEE Transactions on Circuits and Systems I: accepted for publication.
[66] J. Muller, C. Kuttler, B. Hense, M. Rothballer, and A. Hartmann, Journal of Mathematical Biology, **53**, 672 (2006).
[67] J.Dockery and J. Keener, Bulletin of Mathematical Biology, **63**, 95 (2004).
[68] C. Godsil and G. Royle, *Algebraic Graph Theory* (Springer Verlag (New York), 2001).